Free Radical Biology and Medicine 113 (2017) 190–202

Contents lists available at ScienceDirect

Free Radical Biology and Medicine

journal homepage: www.elsevier.com/locate/freeradbiomed

Original article

Redox imbalance due to the loss of mitochondrial NAD(P)-transhydrogenase markedly aggravates high fat diet-induced fatty liver disease in mice

Claudia D.C. Navarro[a], Tiago R. Figueira[a], Annelise Francisco[a], Genoefa A. Dal'Bó[a], Juliana A. Ronchi[a], Juliana C. Rovani[b], Cecilia A.F. Escanhoela[c], Helena C.F. Oliveira[b], Roger F. Castilho[a,*], Anibal E. Vercesi[a,*]

[a] Departamento de Patologia Clínica, Faculdade de Ciências Médicas, Universidade Estadual de Campinas (UNICAMP), 13083-887 Campinas, SP, Brazil
[b] Departamento de Biologia Estrutural e Funcional, Instituto de Biologia, Universidade Estadual de Campinas (UNICAMP), 13083-865 Campinas, SP, Brazil
[c] Departamento de Anatomia Patológica, Faculdade de Ciências Médicas, Universidade Estadual de Campinas (UNICAMP), 13083-887 Campinas, SP, Brazil

ARTICLE INFO

Keywords:
Liver steatosis
Steatohepatitis
Pyruvate dehydrogenase
Nnt mutation
C57BL/6J mouse

ABSTRACT

The mechanisms by which a high fat diet (HFD) promotes non-alcoholic fatty liver disease (NAFLD) appear to involve liver mitochondrial dysfunctions and redox imbalance. We hypothesized that a HFD would increase mitochondrial reliance on NAD(P)-transhydrogenase (NNT) as the source of NADPH for antioxidant systems that counteract NAFLD development. Therefore, we studied HFD-induced liver mitochondrial dysfunctions and NAFLD in C57Unib.B6 congenic mice with ($Nnt^{+/+}$) or without ($Nnt^{-/-}$) NNT activity; the spontaneously mutated allele ($Nnt^{-/-}$) was inherited from the C57BL/6J mouse substrain. After 20 weeks on a HFD, $Nnt^{-/-}$ mice exhibited a higher prevalence of steatohepatitis and content of liver triglycerides compared to $Nnt^{+/+}$ mice on an identical diet. Under a HFD, the aggravated NAFLD phenotype in the $Nnt^{-/-}$ mice was accompanied by an increased H_2O_2 release rate from mitochondria, decreased aconitase activity (a redox-sensitive mitochondrial enzyme) and higher susceptibility to Ca^{2+}-induced mitochondrial permeability transition. In addition, HFD led to the phosphorylation (inhibition) of pyruvate dehydrogenase (PDH) and markedly reduced the ability of liver mitochondria to remove peroxide in $Nnt^{-/-}$ mice. Bypass or pharmacological reactivation of PDH by dichloroacetate restored the peroxide removal capability of mitochondria from $Nnt^{-/-}$ mice on a HFD. Noteworthy, compared to mice that were chow-fed, the HFD did not impair peroxide removal nor elicit redox imbalance in mitochondria from $Nnt^{+/+}$ mice. Therefore, HFD interacted with *Nnt* mutation to generate PDH inhibition and further suppression of peroxide removal. We conclude that NNT plays a critical role in counteracting mitochondrial redox imbalance, PDH inhibition and advancement of NAFLD in mice fed a HFD. The present study provide seminal experimental evidence that redox imbalance in liver mitochondria potentiates the progression from simple steatosis to steatohepatitis following a HFD.

1. Introduction

The increased consumption of fat-rich and energy-dense foods is a nutritional behavior that is associated with a myriad of metabolic, cardiovascular and hepatic diseases of rising worldwide prevalence [1]. Prominent hepatic abnormalities, such as insulin resistance, non-alcoholic fatty liver disease (NAFLD), and increased rates of gluconeogenesis and glucose output can result from a high fat diet (HFD), and their pathophysiological mechanisms have been extensively studied in experimental rodent models [2–5]. Several studies have implicated mitochondrial dysfunctions in the etiology of metabolic and morphological alterations that occur in the liver in response to a HFD [5–8], but a causal relationship is not always clear [5,7,9]. Higher mitochondrial production of reactive species and impaired redox balance have been indicated as events that are involved in the progression from simple steatosis to nonalcoholic steatohepatitis (NASH) [9,10]. Recently, studies have demonstrated the importance of the inhibition of mitochondrial pyruvate dehydrogenase (PDH) in the context of NAFLD by showing that pharmacological or genetic activation of PDH ameliorated the increased hepatic glucose output and the steatosis induced by HFD in mice [3,11,12]. Pyruvate oxidation is relevant in liver mitochondria [3,4], and its decrease seems to cause pyruvate to be channeled into the gluconeogenesis pathway, impairing glucose homeostasis in mice on a HFD [3]. However, a plausible interplay between impaired redox balance and pyruvate oxidation may occur in liver mitochondria following a HFD; the rationale for this hypothesis is presented below.

* Corresponding authors.
E-mail addresses: roger@fcm.unicamp.br (R.F. Castilho), anibal@unicamp.br (A.E. Vercesi).

http://dx.doi.org/10.1016/j.freeradbiomed.2017.09.026
Received 6 June 2017; Received in revised form 30 August 2017; Accepted 26 September 2017
Available online 28 September 2017
0891-5849/

Knowing that reduced NADP is the driving energy source for peroxide removal via the glutathione- and thioredoxin-dependent antioxidant systems [8,13,14] and that its oxidation is associated with the opening of the mitochondrial permeability transition pore (PTP) [15,16], we hypothesized that another consequence of HFD-induced PDH inhibition is redox imbalance and aggravation of NAFLD when the supply of mitochondrial NADPH is not adequately shifted towards sources that are independent of pyruvate oxidation and Krebs cycle flux, such as the enzyme NAD(P)-transhydrogenase (NNT). Previous findings collectively demonstrated that pyruvate oxidation via PDH and downstream Krebs cycle reactions is important for NADPH-dependent peroxide removal because the generated isocitrate sustains NADPH production by NADP-dependent isocitrate dehydrogenase (IDH2) [17,18]. IDH2 is a main source of NADPH, along with NNT in liver mitochondria [17,19,20]. Thus, if pyruvate flux is impaired, concurrent sources of mitochondrial NADPH, particularly NNT, will need to increase their relative contributions to maintain redox balance. NNT is located in the inner mitochondrial membrane and reduces $NADP^+$ at the expense of NADH oxidation and H^+ translocation down the protonmotive force across the inner mitochondrial membrane, thus maintaining NADP in a highly reduced state [13,16]. Interestingly, C57BL/6J mice have a spontaneous mutation of the NNT gene (*Nnt*) [18,21], are apparently more susceptible to HFD-induced metabolic diseases than other substrains [22–24], and are widely used as models of HFD-induced obesity, insulin resistance and NAFLD [2,7,22]. Nonetheless, in addition to *Nnt* mutation, other genetic modifiers could play a role in phenotypic differences between mice substrains [25–31]. As a result of this *Nnt* mutation, liver mitochondria that are devoid of NNT function display a lower peroxide removal capacity as well as other redox abnormalities [17,18]. Therefore, the role of NNT in counteracting HFD-induced redox imbalance linked to PDH inhibition seems a sound and unexplored hypothesis.

We have recently generated congenic C57Unib.B6 mice bearing wild type ($Nnt^{+/+}$) or the mutated ($Nnt^{-/-}$) *Nnt* allele from the C57BL/6J substrain [17]. In the current study, we maintained these congenic mice (C57Unib.B6-$Nnt^{+/+}$, C57Unib.B6-$Nnt^{-/-}$) on a chow diet or a HFD to investigate the role of NNT-dependent mitochondrial redox balance in HFD-induced NAFLD. For comparative purposes, the liver histology of C57BL/6J mice on a HFD was also evaluated because innumerous studies have employed this substrain.

2. Material and methods

2.1. Reagents

The fluorescent probes Calcium Green™-5N and Amplex Red® were purchased from Invitrogen (Carlsbad, California, USA) and dissolved in deionized water and dimethyl sulfoxide (DMSO), respectively. The primary antibodies against PDH-E1α (code # 110330) and serine^{293}-phosphorylated PDH-E1α (code # 177461) were ordered from Abcam (Cambridge, MA, USA). Secondary antibodies conjugated with HRP were purchased from BD Bioscience (rabbit anti-mouse, code # 554002; San Jose, CA, USA) and Cell Signaling (goat anti-rabbit, code # 7074, Beverly, MA, USA). Malic acid, sodium pyruvate, succinic acid, oxaloacetic acid, sodium α-ketoglutarate, glutamic acid, sodium isocitrate, citric acid, palmitoylcarnitine, tert-butyl hydroperoxide (t-BOOH), rotenone, carbonyl cyanide 4-(trifluoromethoxy)phenylhydrazone (FCCP), oligomycin, oxidized nicotinamide adenine dinucleotide phosphate ($NADP^+$), reduced nicotinamide adenine dinucleotide (NADH), adenosine diphosphate (ADP), sodium dichloroacetate, NADP-isocitrate dehydrogenase, peroxidase from horseradish type VIA (HRP), a protease inhibitor cocktail (code P8340) and most other chemicals were obtained from Sigma-Aldrich (Saint Louis, MO, USA). Stock solutions of respiratory substrates, nucleotides and sodium dichloroacetate were prepared in a 20 mM HEPES solution with the pH adjusted to 7.2 using KOH.

2.2. Animals

C57BL/6J mice were obtained from the Campinas University Multidisciplinary Center for Biological Research in Laboratory Animals (CEMIB/UNICAMP, Campinas, Brazil), which breeds a mouse colony that is confirmed to be homozygous for mutated *Nnt* alleles (a 17,814-bp deletion in the *Nnt* gene, resulting in the absence of exons 7–11) [17,18]. A congenic mouse model carrying wild-type or the *Nnt* mutated alleles from the C57BL/6J substrain was recently generated on the genetic background of C57BL/6/JUnib mouse substrain in our laboratory, as detailed in Ronchi et al. [17]. These congenic mice were bred in our department's animal facility and the N7 (the seventh backcrossed generation) was used in this study. The full designations of these congenic mice are C57Unib.B6-$Nnt^{+/+}$ and C57Unib.B6-$Nnt^{-/-}$, which will be referred to by their *Nnt* genotype only (i.e., $Nnt^{+/+}$ and $Nnt^{-/-}$). We ordered the "genome scanning service" from The Jackson Laboratory to analyze four independent samples from N7 congenic mice and two independent samples from C57BL/6J mice (purchased from the local provider) using the "C57BL/6 substrain characterization panel" of 150 validated SNPs; the results indicated that C57BL/6J mice from the local provider exhibited all 150 SNPs identical to The Jackson Laboratory reference C57BL/6J substrain; also, the comparison between C57BL/6J and four mice from our congenic model showed a difference of 28% SNPs. Male mice were kept under standard laboratory conditions (at 20–22 °C and a 12 h/12 h light/dark cycle) with free access to tap water and to either a standard diet or a high fat diet (specified below) in the local animal facility, according to Brazilian guidelines and the "Guide for the Care and Use of Laboratory Animals" from the National Academy of Sciences. Male mice were chosen because they are more susceptible to HFD-induced NAFLD than female (which are protected by estrogens) and develop markers of inflammation like humans with NASH [32,33]. The mice were euthanized by cervical dislocation prior to harvesting the liver for further analysis. The use of mice and the experimental protocols were approved by the local Committee for Ethics in Animal Research (CEUA-UNICAMP, approval number 3914-1). The animal procedures comply with national Brazilian guideline number 13 for "Control in Animal Experiments", published on September 13th, 2013 (code 00012013092600005, available at ⟨http://portal.in.gov.br/verificacao-autenticidade⟩).

2.3. High fat diet (HFD) treatment

One-month-old congenic and C57BL/6J male mice were randomly assigned to groups fed either the standard diet (Chow, total energy of 3.9 kcal/g, 5% fat, 12% of total calories from fat) from Nuvital (Nuvilab CR1, Nuvital, Colombo, PR, Brazil) or a HFD from PragSoluções (Hyperlipidic diet, PragSoluções biociências, Jaú, SP, Brazil). The composition of the HFD was as follows: 31% lard fat, 20% casein, 13% dextrinized cornstarch, 12% cornstarch, 10% sucrose, 5% microcrystalline cellulose, 4% soybean oil, 3.5% mineral mix AIN 93 G, 1% vitamin mix AIN 93, 0.3% L-cysteine, 0.25% choline bitartrate, and 0.0028% butylhydroxytoluene (also present as a preservative in the standard chow). The caloric content of this HFD is 5.3 kcal/g, from which ~60% of total energy were derived from fats (90% from lard fat and 10% from vegetable oil). Mice were maintained on a standard diet or HFD for 20 weeks prior to being sacrificed for liver removal and use in histology or mitochondrial isolation.

3. Measurements

3.1. Liver histology

Approximately 3 mm-sided fragments of the two largest liver lobules were cut and placed in 10% formaldehyde for 24 h at room temperature. Then, tissue samples were embedded in paraffin before being sectioned (5 μm thick slices). These liver slices were placed on

glass slides in a 40 °C water bath and then were dried at 60 °C in an incubator for 20 min. Next, the slides were subjected to conventional hematoxylin plus eosin or picrosirius red staining protocols. An experienced pathologist performed blind evaluations of stained sections under an optical microscope to grade the following abnormalities: ballooning (a grade of 3 was assigned when associated with Mallory's hyaline), macrovesicular steatosis, acinar inflammation and portal inflammation (on a scale of 0–3), and fibrosis (on a scale of 0–4) (fibrosis grading was based on Picrosirius red staining); microvesicular steatosis was marked as absent [0] or present [1]. The sum of these grades provides an overall NAFLD activity score between 0 and 17. As proposed by Kleiner et al. [34], a NAFLD activity score between 0 and 8 is obtained if only the grades of ballooning injury (on a scale of 0–2), steatosis (on a scale of 0–3), and acinar inflammation (on a scale of 0–3) are accounted for human NAFLD diagnosis purposes.

3.2. Content of liver triglycerides

Lipids were extracted from livers by following a modified Folch's method. Briefly, approximately 60 mg of diced wet liver was homogenized in 3 mL of organic solvents (2 mL chloroform plus 1 mL methanol), filtered through fat-free paper and left to dry overnight inside a fume hood at room temperature. Then, half a milliliter of an amphiphilic medium (100 mM KH_2PO_4, 50 mM NaCl, 5 mM cholic acid, 0.1% Triton X-100, pH 7.4) was added to each tube containing the dried, extracted lipids. Then, the triglyceride level of this lipid mixture was measured by a commercial enzymatic-colorimetric kit (Roche-Hitachi, Germany) to calculate the total triglyceride content.

3.3. Mitochondrial isolation and incubation conditions

Mitochondria were isolated from mice livers by conventional differential centrifugation, as detailed described previously [35]. Because of the high lipid content in mouse livers following the HFD, livers from all mouse groups were homogenized and processed in mitochondrial isolation medium (250 mM sucrose, 10 mM HEPES and 0.5 mM EGTA) supplemented with 1 g/L bovine serum albumin until the second centrifugation step. Measurements of respiration, hydrogen peroxide release, Ca^{2+} retention capacity and the redox state of NAD(P) in suspensions of intact mitochondria were performed at 28 °C with continuous magnetic stirring in 2 mL of standard reaction medium (125 mM sucrose, 65 mM KCl, 2 mM KH_2PO_4, 1 mM $MgCl_2$, 10 mM HEPES buffer with the pH adjusted to 7.2 with KOH). The addition of various respiratory substrates and the presence of other chemicals are specified in the figure legends. Because of their time consuming characteristics, the *in vitro* protocols with isolated and functional mitochondria were performed with two groups from the same *Nnt* genotype in each experimental run (always comparing chow *vs.* HFD).

3.4. Enzymes activities

The activities of the enzymes aconitase, NADP-dependent isocitrate dehydrogenase (IDH2) and citrate synthase were spectrophotofluorometrically assayed in the isolated mitochondrial suspensions according to previously used protocols [18,36] that are described in the Supplementary material.

3.5. Oxygen consumption

Mitochondria were suspended (0.5 mg/mL) in 1.4 mL of standard reaction medium supplemented with 200 μM EGTA and 5 mM each of malate, glutamate, pyruvate, and α-ketoglutarate. Respiration was measured using a Clark-type electrode (YSI Co., Yellow Spring, OH, USA) in a temperature-controlled chamber equipped with a magnetic stirrer. After measuring the resting O_2 consumption, respiration linked to oxidative phosphorylation (also known as state 3) was elicited by the addition of 150 μM of ADP. Then, 1 μg/mL of oligomycin was added to cease the phosphorylation by ATP synthase, slowing down oxygen consumption. Finally, 80 nM of FCCP was added to promote maximal uncoupled respiration.

3.6. Mitochondrial hydrogen peroxide (H_2O_2) release

Mitochondria were suspended (0.5 mg/mL) in 2 mL of standard reaction medium supplemented with 300 μM EGTA, 10 μM Amplex Red®, 1 U/mL horseradish peroxidase with malate (2.5 mM) plus pyruvate (5 mM) as respiratory substrates. In this condition, the H_2O_2 released from mitochondria causes the oxidation of Amplex Red® and the formation of its fluorescent product, resorufin, which was monitored over time in a spectrofluorometer (Hitachi F-4500, Tokyo, Japan) operating with slit widths of 2.5 nm and at 563 and 587 nm for the excitation and emission wavelengths, respectively.

3.7. Assessment of Ca^{2+}-induced opening of the mitochondrial permeability transition pore (PTP)

Mitochondria were suspended (0.5 mg/mL) in the standard reaction medium supplemented with 15 μM EGTA, 0.2 μM of a calcium indicator (Calcium Green™-5N) and respiratory substrates (2.5 mM malate plus 5 mM pyruvate or 5 mM succinate plus 1 μM rotenone). The fluorescence was continuously monitored in a spectrofluorometer (Hitachi F-4500, Tokyo, Japan) using excitation and emission wavelengths of 506 and 532 nm, respectively, and slit widths of 5 nm. Repeated pulses of $CaCl_2$ additions (2.5 μM or 15 μM for malate plus pyruvate or succinate plus rotenone conditions, respectively) were performed every 3 min after the addition of mitochondria to the system. The number of $CaCl_2$ pulses added prior to the start of Ca^{2+} release by mitochondria into the medium was measured as an index of the susceptibility to Ca^{2+}-induced PTP.

3.8. Redox state of mitochondrial nicotinamide nucleotides (NAD(P))

Mitochondria were suspended (0.5 mg/mL) in the standard reaction medium supplemented with 300 μM EGTA and either malate (2.5 mM) plus pyruvate (0.1 or 5 mM) or malate (2.5 mM) plus palmitoylcarnitine (15 μM) as respiratory substrates (specific concentrations and the addition of other reagents are indicated in figure legends). The changes in the redox state of NAD(P) were monitored in a spectrofluorometer (Hitachi F-4500, Tokyo, Japan) using excitation and emission wavelengths of 366 and 450 nm, respectively, and slit widths of 5 nm. Worthnoting, only the reduced form of NAD(P) exhibits a strong endogenous fluorescence signal. The mitochondrial capacity to remove peroxide was assessed by challenging the mitochondrial peroxide-metabolizing system supported by NADPH with exogenous t-BOOH, an organic peroxide that is metabolized via the glutathione and thioredoxin peroxidase/reductase systems (but not by catalase) at the expense of NADPH [37,38]. The mitochondrial contents of reduced NADP (NADPH) were enzymatically determined using a commercially available kit according to manufacturer's instructions (#G9071, Promega, Madison, USA).

3.9. PDH expression and phosphorylation state

The final pellet of isolated mitochondrial fraction was suspended in a medium containing phosphatase and protease inhibitors (50 mM Tris, 150 mM NaCl, 1 mM EGTA, 1 mM Na_3VO_4, 1 mM NaF, 1% Tween 20, 1% protease inhibitor cocktail, and pH 7.4). Then, the samples were diluted in standard Laemmli buffer before being subjected (50 μg of total proteins per lane) to 8% *polyacrylamide gel electrophoresis* (PAGE). The resolved proteins were transferred (120 V for 90 min, on ice) from the gel to a nitrocellulose membrane (0.45 μm, from Bio-Rad, Hercules, CA). Following the blocking of membrane with 5% dried milk, the

membrane was washed and incubated overnight at 4 °C with 1:1000 diluted primary antibodies against PDH-E1α (a subunit of the PDH complex) or serine^{293}-phosphorylated PDH-E1α. After washing the membrane free of primary antibodies, it was incubated with HRP-conjugated secondary antibodies (1:10000 diluted) for 1 h at room temperature. Finally, the membrane was washed and incubated with a enhanced chemiluminescence reagent (SuperSignal West Pico, Thermo Fisher, Waltham, MA, USA) and the luminescence signals were detected in a digital instrument (UVITEC, Cambridge, UK).

4. Statistical analyses

The results are shown as representative and/or as the mean ± SEM (individual values and medians are reported for non-parametric data). Sample sizes are indicated in figure legends. Two-way ANOVA followed by Bonferroni as a post-hoc was used to test differences between groups for most data, with the exception of data shown in Fig. 4, which were tested with Wilcoxon (when groups were correlated) or Mann-Whitney tests. The level of significance was set at $P \leq 0.05$.

5. Results

In the present study, we initially evaluated HFD-induced hepatic alterations in C57BL/6J and congenic mice bearing the *Nnt*$^{+/+}$ or *Nnt*$^{-/-}$ alleles. Histopathological and biochemical analyses revealed that twenty weeks of a HFD promoted NAFLD in all three groups of mice, i.e., the *Nnt*$^{+/+}$, *Nnt*$^{-/-}$ and C57BL/6J mice (Figs. 1 and 2). However, mice groups lacking a functional NNT due to the *Nnt* mutation (*Nnt*$^{-/-}$ and C57BL/6J mice) exhibited increased frequency of ballooning injury, micro and macrovesicular steatosis of higher grades and elevated contents of liver triglycerides than *Nnt*$^{+/+}$ mice. The sums of the scores presented in panels A to D in Fig. 2 (the median ± interquartile range values were 3 ± 2, 7 ± 0 and 8 ± 2 for *Nnt*$^{+/+}$, *Nnt*$^{-/-}$ and C57BL/6J mouse groups on a HFD, respectively) were significantly ($P \leq 0.05$, determined by Kruskal-Wallis ANOVA with Dunns as post-hoc) higher in *Nnt*$^{-/-}$ and in C57BL/6J than in *Nnt*$^{+/+}$ mice. The NAFLD activity score, as proposed by Kleiner et al. [34], indicated that most of *Nnt*$^{+/+}$ mice developed simple steatosis following the HFD, while most of *Nnt*$^{-/-}$ exhibited scores indicative of NASH, an aggravated form of NAFLD. Interestingly, compared to *Nnt*$^{-/-}$ mice on the same diet, C57BL/6J mice displayed worsened hepatic alterations when fed HFD, as evidenced by ~50% higher liver triglyceride contents (Fig. 1), as well as increased grades of acinar/portal inflammation and fibrosis (Fig. 2**E** and **F**). NNT has been previously shown to play a main role in mitochondrial redox homeostasis by supplying NADPH, which in turn drives reductive processes, such as enzymatic peroxide removal through the glutathione and thioredoxin dependent systems [17]. Therefore, these hepatic phenotypes of *Nnt*$^{+/+}$, *Nnt*$^{-/-}$ and C57BL/6J mice fed chow or a HFD provided proof of the concept that mitochondrial redox imbalance aggravates HFD-induced NAFLD. Following this initial observation, experiments were designed to assess mitochondrial redox balance and related biochemical events that delineated the worsening of NAFLD upon the interaction between *Nnt* mutation and a HFD. To this end, isolated liver mitochondria were obtained from *Nnt*$^{+/+}$ and *Nnt*$^{-/-}$ mice that were given either standard chow or a HFD and were studied under suitable conditions.

Resting and ADP-stimulated mitochondrial respiration, supported by a cocktail of complex I-linked substrates and in the absence of free Ca^{2+}, did not differ among the groups of congenic mice, given either chow or a HFD (Supplementary material).

The rate of H_2O_2 release from mitochondria was increased by the HFD in *Nnt*$^{-/-}$ mice only, indicating that this redox alteration was underpinned by the interaction between HFD and the *Nnt* mutation (Fig. 3**A, B**). Because the activity of aconitase relies on the redox state of its ferrous group, the activity of this enzyme is a sensitive marker of redox balance in mitochondria [36]. Compared to chow-fed *Nnt*$^{+/+}$, *Nnt*$^{-/-}$ mice under chow or a HFD presented with approximately 15% and 50% lower aconitase activities, respectively (Fig. 3**C**). Notably, the HFD alone did not affect aconitase activity, but the decrease was greater upon the interaction between the HFD and the *Nnt* mutation. IDH2 in the Krebs cycle, as well as NNT, have high activities for reducing $NADP^+$ to NADPH in the mitochondrial matrix [17]. Presumably, the relative importance of IDH2 may be augmented in the absence of NNT and/or in response to oxidative stress. Data shown in Fig. 3**D** indicated that the activity of IDH2 was significantly upregulated only in *Nnt*$^{-/-}$ mice given a HFD; there were non-significant trends of increased IDH2 activity in response to *Nnt* mutation or HFD alone.

The Ca^{2+}-induced opening of the mitochondrial permeability transition pore (PTP) is a redox-sensitive event that may result in bioenergetic dysfunction, cellular injury and apoptosis [14]. The assessment of Ca^{2+}-induced mitochondrial Ca^{2+} release that occurs via PTP pore opening suggested divergent effects between *Nnt* mutation and HFD (Fig. 4). As expected, in mice fed a chow diet [18], the susceptibility to Ca^{2+}-induced PTP opening was higher in *Nnt*$^{-/-}$ compared to *Nnt*$^{+/+}$ mice when mitochondria respired on succinate in the presence of rotenone (Fig. 4**C, D** and **F**), but not when malate and pyruvate were the respiratory substrates (Fig. 4**A, B** and **E**). Surprisingly, HFD decreased the susceptibility to Ca^{2+}-induced PTP opening in mitochondria from *Nnt*$^{+/+}$ mice, regardless of the respiratory substrates supplied. The *Nnt* mutation profoundly changed the effect of the HFD on this variable, since mitochondria from *Nnt*$^{-/-}$ mice on a HFD exhibited higher susceptibility to Ca^{2+}-induced PTP opening than mitochondria from either *Nnt*$^{-/-}$ or *Nnt*$^{+/+}$ mice on a chow diet. The decreased susceptibility to Ca^{2+}-induced PTP opening in mitochondria from *Nnt*$^{+/+}$ mice following a HFD seems not to be related to mitochondrial selection during the isolation procedure, since the recovery of mitochondria (citrate synthase activity) from the total liver was similar between diet treatments in *Nnt*$^{+/+}$ mice (chow diet: 47 ± 3%, N = 4; HFD: 40 ± 4%, N = 6).

The *Nnt* mutation itself was previously shown to reduce the mitochondrial capacity to metabolize peroxide [17,18], and according to our stated hypothesis, such dysfunction could be exacerbated by a HFD. The mitochondrial capacity to remove a peroxide load was first evaluated during the resting respiratory state (i.e., in the absence of exogenous ADP) sustained by malate and pyruvate as substrates (Fig. 5**A, B** and **E**). These data clearly demonstrated that HFD decreased the mitochondrial capacity to remove peroxide in *Nnt*$^{-/-}$ mice only, while *Nnt*$^{+/+}$ mice were protected against this deleterious effect caused by the HFD. In the absence of an NADPH supply via NNT, substrate oxidation through the Krebs cycle is the source of NADPH that sustains NADPH-dependent peroxide removal in the mitochondrial matrix [17,18]. Thus, mitochondria from *Nnt*$^{-/-}$ mice on a HFD were presumed to exhibit impaired oxidation of the available malate and pyruvate substrates. In the following experiment (Fig. 5**C, D** and **E**), a peroxide removal assay was performed in the presence of exogenous ADP (i.e., the phosphorylating state). Exogenous ADP exerts profound effects on mitochondrial metabolism and peroxide removal [17], favoring NADPH supply via substrate oxidation because ADP activates dehydrogenases such as PDH, stimulates oxidative phosphorylation, and increases substrate flux through the Krebs cycle. The peroxide removal rate in the presence of ADP did not differ between *Nnt*$^{-/-}$ and *Nnt*$^{+/+}$ mice given either a chow or a HFD. This indicated that NNT does not contribute to peroxide removal under the respiratory condition of ADP phosphorylation sustained by malate and pyruvate as substrates, corroborating our previous findings from studying mice given a standard chow diet [17]. The time to remove peroxide in the presence of ADP was slightly and significantly increased by the HFD in mitochondria from *Nnt*$^{+/+}$ mice only (Fig. 5**E**). Curiously, *Nnt*$^{-/-}$ mice did not exhibit this alteration, which seems to be related to the fact that on a HFD, this genotype developed higher IDH2 activity, and thus was perhaps better adapted to handle peroxide removal in an NNT-independent manner. The effects of a HFD, *Nnt* mutation and ADP on peroxide removal are summarized for

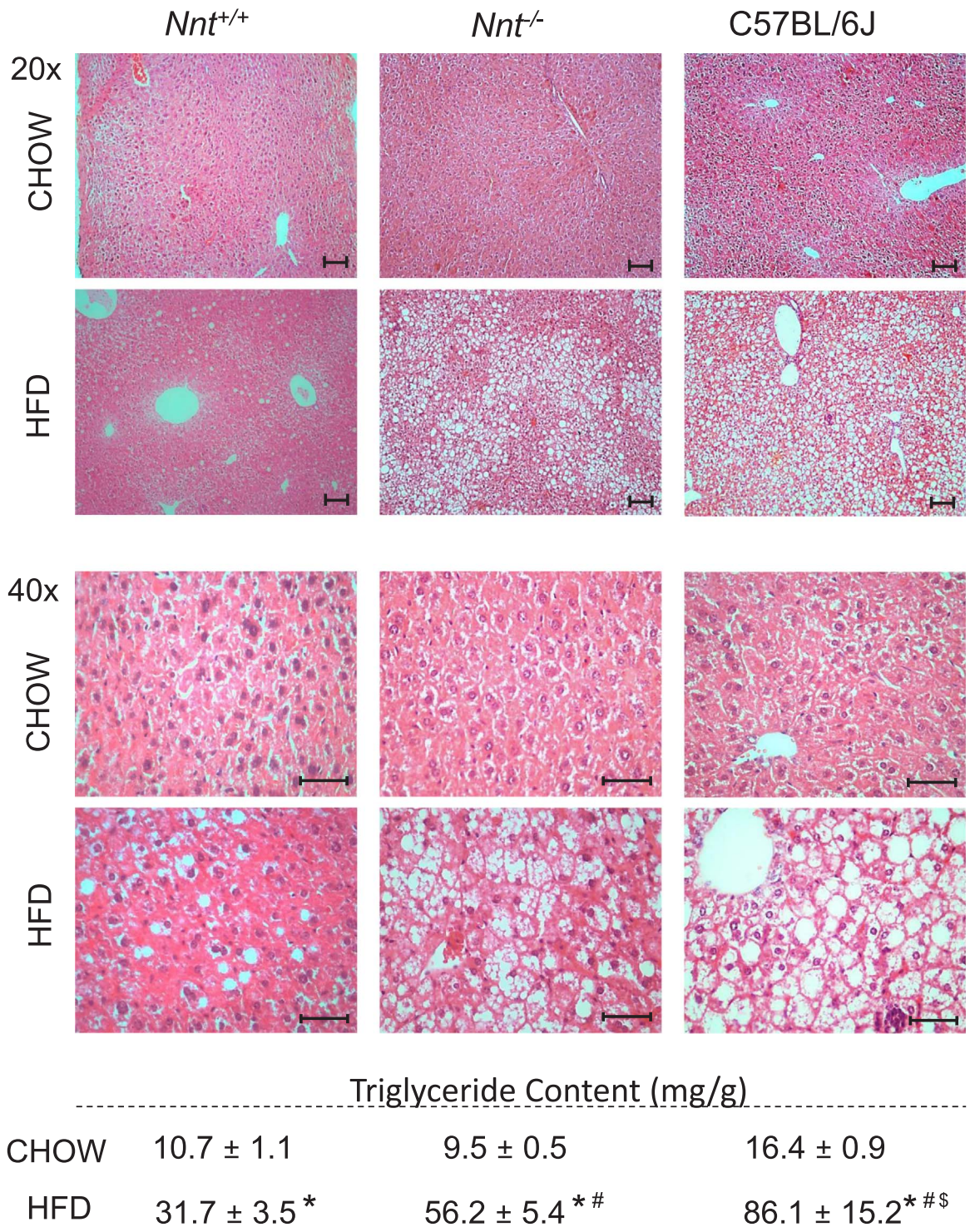

Fig. 1. Histological characterization of fatty liver disease and triglycerides contents in livers from $Nnt^{+/+}$, $Nnt^{-/-}$ and C57BL/6J mice following a high fat diet (HFD). Section (5 μm) of liver were stained with hematoxylin and eosin and observed using an optical microscope (20× objective, scale bar = 100 μm; 40× objective; scale bar = 50 μm) for the evaluation of abnormalities characterizing simple steatosis and nonalcoholic steatohepatitis; N = 5–7. The content of liver triglyceride (mg/g of wet liver) was biochemically determined and the means ± SEM (N = 5–14) of each mice genotype on both diets are reported below the corresponding column of images. Control groups were fed with a chow diet. $^{*}P \leq 0.01$ *vs.* genotype-matched chow-fed mice; $^{\#}P \leq 0.01$ *vs.* $Nnt^{+/+}$ on a HFD; $^{\$}P \leq 0.01$ *vs.* $Nnt^{-/-}$ on a HFD.

better visualization in an integrated graph shown in Fig. 5**F**. Overall, these results demonstrated marked effects of exogenous ADP as it nearly abolished the entire extent of the HFD deleterious effects (Fig. 5**B** and **E**) on the mitochondrial capacity to remove peroxide in $Nnt^{-/-}$ mice (Fig. 5**D** and **E**).

Because the HFD effects on the ADP-induced changes in peroxide removal from the resting state were much larger in $Nnt^{-/-}$ than in $Nnt^{+/+}$ mice (~150% *vs.* ~ 15%) (Fig. 5**F**), we designed new protocols (Fig. 6) to investigate whether PDH was the molecular target responsible for the modulations of peroxide removal by the interaction between HFD and ADP. Interestingly, when pyruvate was replaced by palmitoylcarnitine, thus feeding acetyl-CoA into the Krebs cycle independently of PDH, the peroxide removal by mitochondria from both $Nnt^{+/+}$ and $Nnt^{-/-}$ mice matched each other and was not affected by a

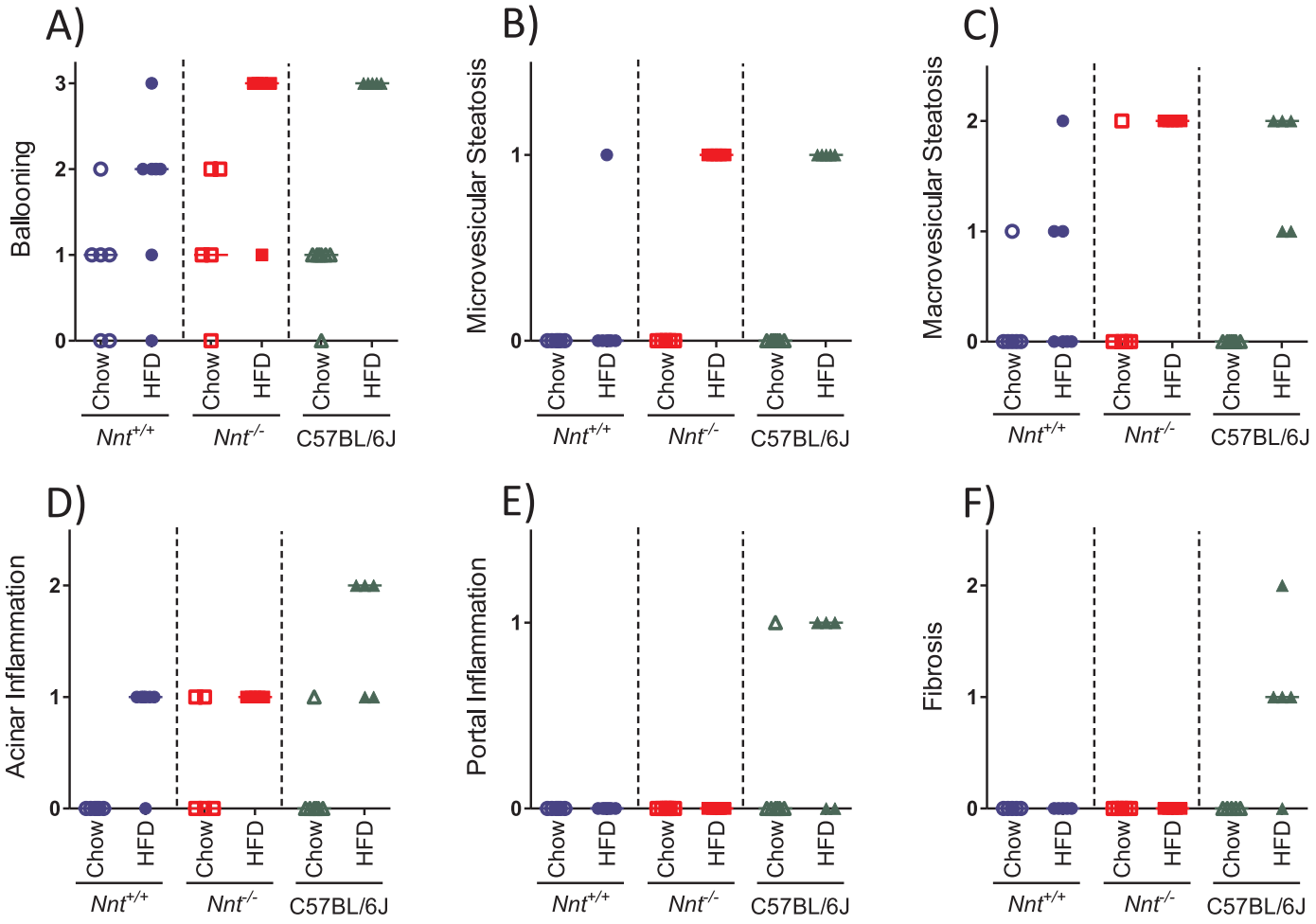

Fig. 2. Grading of pathological alterations in livers from *Nnt*$^{+/+}$, *Nnt*$^{-/-}$ and C57BL/6J mice under a chow or a high fat diet (HFD): loss of NADP-transhydrogenase caused the progression from simple steatosis to nonalcoholic steatohepatitis. The following hepatic abnormalities were graded according to a proposed [34] non-alcoholic fatty liver disease activity score: ballooning (a grade of 3 was assigned when associated with Mallory's hyaline), macrovesicular steatosis, acinar inflammation and portal inflammation were scored on a scale of 0–3, and fibrosis from 0 to 4 (the latter was based on Picrosirius red-staining); microvesicular steatosis was marked as absent (0) or present (1). The higher the grade, the worse is the abnormality. Graphs in panels A-F show individual data.

HFD (Fig. 6**A** and **B**). Then, definitive evidence that decreased pyruvate oxidation through PDH was hampering peroxide removal by mitochondria from *Nnt*$^{-/-}$ mice on a HFD were obtained by using dichloroacetate (DCA) to activate PDH, in combination with high (5 mM) or limiting (0.1 mM) pyruvate concentrations (Fig. 6**C** to **F**). The PDH activation by DCA completely reversed the deleterious effects of the HFD on peroxide removal by mitochondria from *Nnt*$^{-/-}$ mice, while mitochondria from chow-fed *Nnt*$^{-/-}$ or from *Nnt*$^{+/+}$ mice on both diets were not sensitive to DCA (Supplementary material). The stimulatory effects of DCA on peroxide removal by mitochondria from *Nnt*$^{-/-}$ mice were clearly larger when pyruvate oxidation was disfavored in the low pyruvate concentration condition (0.1 mM; Fig. 6**F**), adding to the evidence that HFD promoted PDH inhibition, which in turn decreased pyruvate flux and NADPH-dependent peroxide removal in *Nnt*$^{-/-}$ mice liver mitochondria. We additionally quantified the contents of reduced NADP following t-BOOH addition to mitochondria from *Nnt*$^{-/-}$ mice on a HFD, under the experimental conditions depicted in Figs. 5D, 6A and 6C. At a given time-point following t-BOOH addition to the system, NADPH contents were back to control levels (i.e. those in absence of t-BOOH) only when ADP or DCA were present in the condition of pyruvate plus malate as substrate or when pyruvate was replaced by palmitoylcarnitine as the source of acetyl-CoA for Krebs cycle, a pathway that bypass PDH (Table 1).

Previous studies have shown, mostly in C57BL/6J mice, that lipid overload leads to the phosphorylation of PDH E1α subunits at serine residues by PDH kinases [3,4,39,40], a classical covalent modulation that inhibits PDH activity [41]. We assessed the levels of both total and serine^{293} phosphorylated PDH E1α subunits by western blot (Fig. 7). The expression levels of the PDH E1α subunit were not changed by either HFD or *Nnt* mutation. In contrast, the levels of PDH E1α subunits phosphorylated at serine^{293} were increased by the HFD in *Nnt*$^{-/-}$ mice only. Thus, the calculated ratio of phosphorylated to total PDH E1α subunits, an inhibitory modulation, was higher in *Nnt*$^{-/-}$ mice on a HFD compared to other groups (Fig. 7**F**).

Given the above results concerning PDH phosphorylation and the effects of the PDH activator DCA on peroxide removal in mitochondria from *Nnt*$^{-/-}$ mice on a HFD, the levels of phosphorylated PDH E1α subunits were probed in suspensions of *Nnt*$^{-/-}$ mitochondria following 5 min in vitro incubation with DCA (under conditions identical to that of Fig. 6**C**) by western blot (Supplementary material). The results indicated that DCA promptly promoted the desphosphorylation of PDH, thus corroborating the interpretation that reactivation of PDH by DCA stimulated peroxide removal in mitochondria from *Nnt*$^{-/-}$ mice on a HFD (Fig. 6**C**).

A graphical summary of the effects of HFD, *Nnt* mutation, and their interaction on selected variables is presented in a radar chart (Fig. 8). This chart was built with the average data presented in previous figures to provide an overview of the main findings from the present study. This chart facilitates the visualization that the *Nnt* mutation interacts with HFD to alter several variables, causing an impairment of pyruvate-

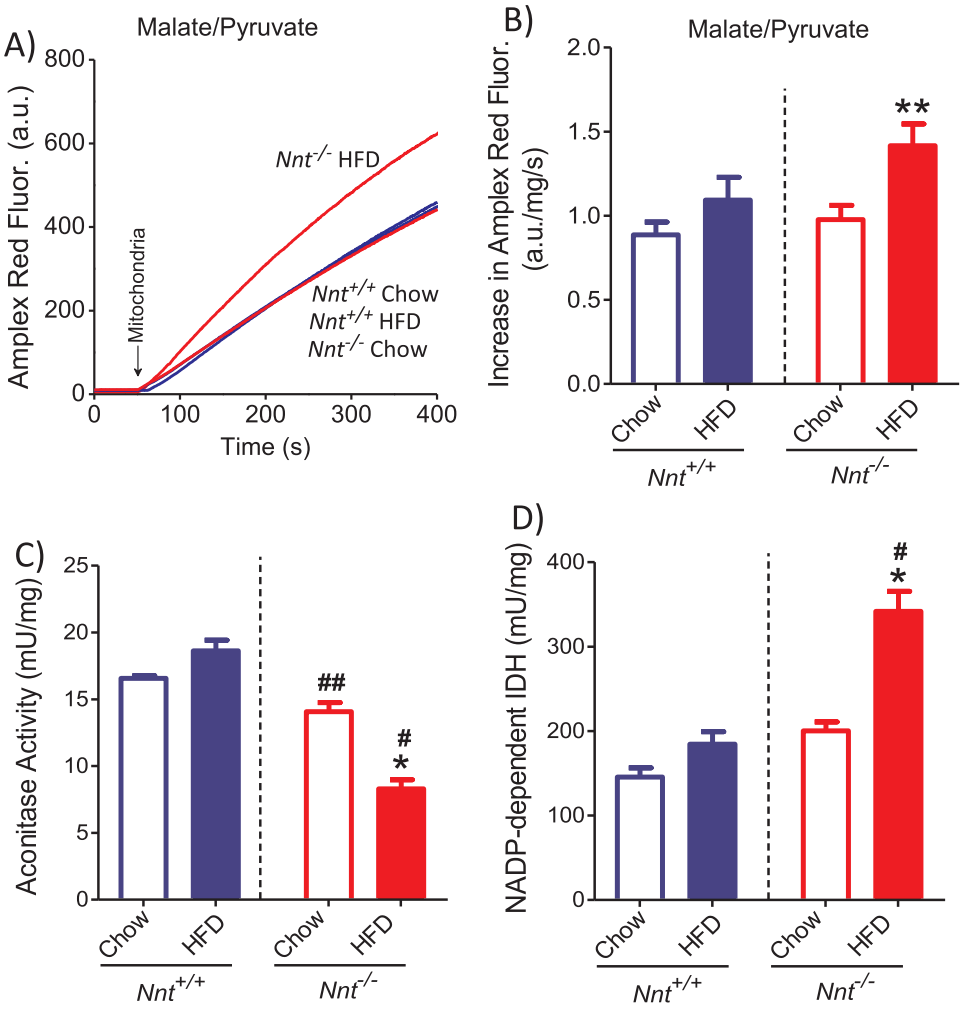

Fig. 3. A high fat diet (HFD) increased the mitochondrial release of H_2O_2 and changed the activities of aconitase and IDH2 in *Nnt*$^{-/-}$ mice only. The release of H_2O_2 from mitochondria was assessed with the fluorescent probe Amplex Red® in the presence of 2.5 mM malate and 5 mM pyruvate as substrates, according to representative traces that are shown in panel A (a sample of isolated mitochondria (0.5 mg/mL) was added to the system where indicated by the arrow). The mean (+ SEM) rate of increase in fluorescence due to Amplex Red oxidation into resorufin are shown in panel B (N = 5–8). The maximal activities of aconitase (an enzyme sensitive to the mitochondrial oxidative balance) and NADP-dependent isocitrate dehydrogenase (IDH2, a concurrent NADPH source in the mitochondrial matrix) were determined in stock suspensions of isolated mitochondria, with their mean (+ SEM) values shown in panels C (N = 6–10) and D (N = 10–17). $^{**}P \leq 0.05$, $^{*}P \leq 0.01$ *vs.* genotype-matched chow-fed mice; $^{\#\#}P \leq 0.05$, $^{\#}P \leq 0.01$ *vs.* *Nnt*$^{+/+}$ mice given the same diet.

supported peroxide removal in liver mitochondria, mitochondrial redox imbalance and the exacerbation of NAFLD activity. The only variable not exhibiting an effect was the "Increase in time to scavenge peroxide in the ADP presence state"; particularly in this experimental condition, PDH can be reactivated and the NNT reaction is thermodynamically disfavored, which results in null contribution of NNT to NADPH-dependent peroxide removal [17], thus, NADPH supply will rely on pyruvate oxidation.

6. Discussion

Mitochondrial redox imbalance has been generally considered to be an important feature of HDF-induced NAFLD and is implicated in the progression of simple liver steatosis to NASH [7,9]. Despite systemic treatments with a variety of antioxidants appear to ameliorate liver steatosis and damage in NAFLD [10,42], the role that oxidative stress in the mitochondrial compartment plays in NAFLD pathophysiology remains incompletely understood. In the current study, using a congenic NNT-null mice model (with genetically suitable controls), we showed that the disruption of NADPH-dependent peroxide removal in mitochondria aggravated the severity of mitochondrial redox imbalance and NAFLD following a HFD, causing the progression from simple steatosis to NASH (Figs. 1 and 2). It is worth noting that the C57BL/6J mice on a HFD exhibited worse hepatic injuries (e.g., fibrosis, acinar and portal inflammation) than *Nnt*$^{-/-}$ congenic mice given the same diet (Figs. 1 and 2), mice which carry the related C57BL/6JUnib genetic background (there are 28% of difference between our congenic mice and the C57BL/6J substrain in a marker panel of 150 single nucleotide polymorphism, see the Material and Methods section). Thus, C57BL/6J mice likely possess other genetic modifiers [26] in addition to their *Nnt* mutation that may explain their aggravated NAFLD phenotype when on a HFD, but we are not aware of any other known genetic modifier that has been experimentally established between the two studied C57BL/6 mice substrains. Other studies have compared metabolic responses of different substrains of C57BL/6 mice to HFDs [23,28,29]. Despite previous direct comparisons between mice substrains that are wild type and mutant for *Nnt* (e.g. C57BL/6N-*Nnt*^{WT} vs. C57BL/6J-*Nnt*^{MUT}), questions remains as to whether the *Nnt* genotype was indeed the unique determinant of the outcomes that eventually differed between mice substrains. It must be reminded that there are significant genetic differences between C57BL/6 mice substrains that can modify the development of complex phenotypes in living animals [43,44], such as glucose metabolism, obesity and fatty liver disease following a HFD [23,28,29]. Indeed, our results regarding HDF-induced NAFLD in *Nnt*$^{-/-}$ and C57BL/6J mice reinforce the theoretical concern about the need of using genetically suitable control mice. This is the first study that used genetically suitable control mice to investigate the role of NNT in the development of NAFLD following a HFD. Therefore, our data shed light on the critical evaluation of research findings from different mice substrains that carry distinct *Nnt* genotypes.

The oxidation of NADH, isocitrate, malate and glutamate by NNT, IDH2, NADP-dependent malic enzymes and glutamate dehydrogenase, respectively, are the known sources of NADPH that sustains reductive functions such as peroxide and xenobiotic removal in liver mitochondria, with NNT and IDH2 exhibiting the highest activities [17]. Under most respiratory conditions, NNT supported the largest portion of

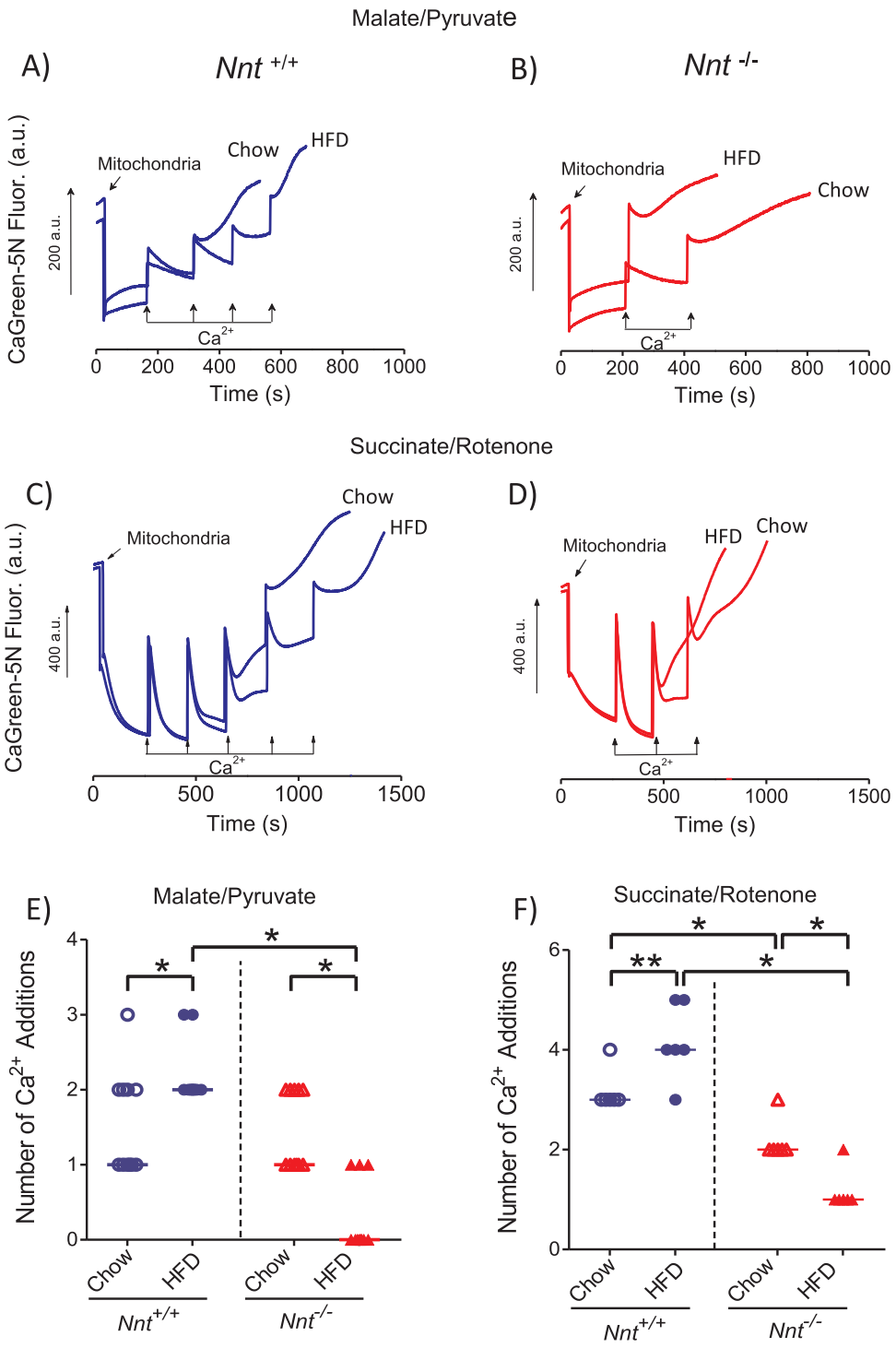

Fig. 4. The *Nnt* genotype modifies the effects of a high fat diet (HFD) on Ca^{2+}-induced mitochondrial permeability transition pore (PTP) opening. Mitochondria (0.5 mg/mL) were incubated in standard reaction medium supplemented with a fluorescent Ca^{2+} probe (0.2 μM Calcium Green™-5N), 15 μM EGTA and respiratory substrates (2.5 mM malate plus 5 mM pyruvate or 5 mM succinate plus 1 μM rotenone). After the addition of mitochondria to the system, Ca^{2+}-induced Ca^{2+} release as a consequence of the opening of PTP was assessed by adding consecutive pulses of Ca^{2+} (2.5 μM and 15 μM for malate plus pyruvate or succinate plus rotenone conditions, respectively) until overt Ca^{2+} release from mitochondria was observed, as depicted in representative traces in panels A to D. Panels A-B and C-D are, the malate plus pyruvate or the succinate plus rotenone conditions, respectively. The individual and median numbers of Ca^{2+} pulses added prior the release of Ca^{2+} from mitochondria of each group are shown in panels E (N = 11) and F (N = 5–6). Brackets in panels E and F denote significant differences between groups ($^{**}P \leq 0.05$, $^{*}P \leq 0.01$).

NADPH-dependent peroxide removal in liver mitochondria from chow-fed mice [17]. The mitochondrial supply of NADPH via non-NNT sources relies on the oxidation of carbon substrates and is expected to be thermodynamically disfavored under conditions of low NAD^+ availability, such as in western diets [45] or respiratory inhibition [13,17]. With this in mind, the present data provides evidence that NNT plays a pivotal role in maintaining redox homeostasis in liver mitochondria challenged by a chronic HFD. Decreased aconitase activity, an endogenous marker of oxidative imbalance, and PDH inhibition primarily arose due to the combination of the *Nnt* mutation and HFD (Figs. 3**C** and 7**F**). This inhibition of PDH, as determined by western blot and functional assessment (Fig. 6), caused the impairment of pyruvate-supported peroxide removal (Fig. 5**B**). In the absence of NNT, pyruvate oxidation through PDH will be important for mitochondrial peroxide removal because it feeds acetyl-CoA into Krebs cycle, thus, forming isocitrate to support $NADP^+$ reduction to NADPH by IDH2. Therefore, in the absence of NNT function, an amplifying cycle between redox imbalance-induced PDH inhibition and PDH inhibition-induced redox imbalance seems to underpin the worsened phenotype of NAFLD induced by the HFD (Figs. 1 and 2).

Despite probing the inhibitory phosphorylation of PDH E1-α subunit at serine[293], which was not identified in $Nnt^{+/+}$ mice mitochondria following HFD (Fig. 7**F**), we obtained an indirect evidence that pyruvate flux through liver PDH was slightly inhibited in this mouse

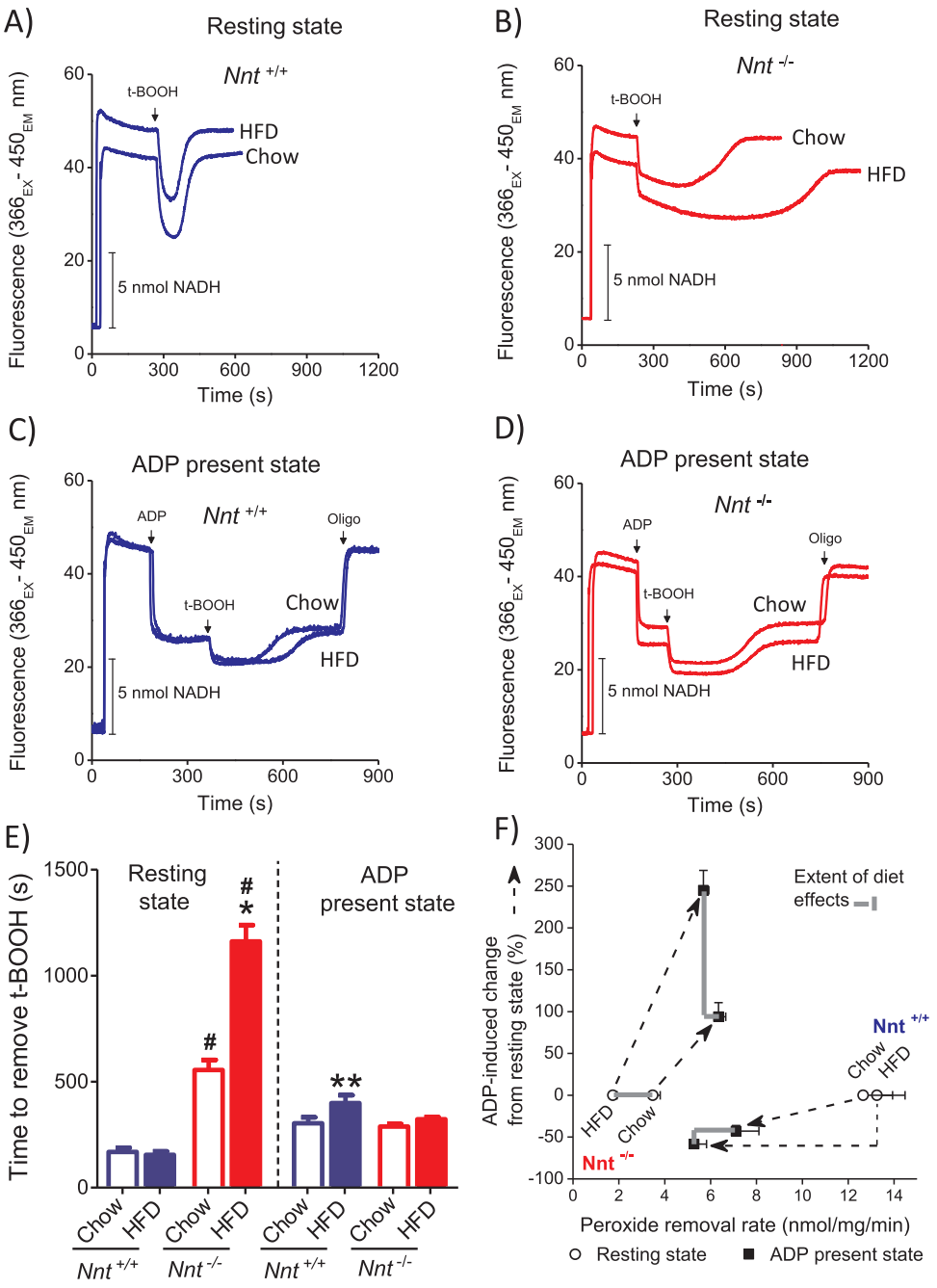

Fig. 5. A high fat diet (HFD) aggravated the already impaired malate/pyruvate supported-mitochondrial peroxide removal in *Nnt*$^{-/-}$ mice: ADP-induced oxidative phosphorylation rescued these abnormalities. The endogenous fluorescence of NAD(P) in the reduced state was continuously monitored over time in mitochondria incubated in standard reaction medium supplemented with 300 μM EGTA and 2.5 mM malate plus 5 mM pyruvate as respiratory substrates. The respiratory condition was maintained in the resting state (panels A and B) or ADP was added to induce oxidative phosphorylation (panels C and D). According to the representative traces shown in panels A to D, a sample of isolated mitochondria (0.5 mg/mL) and 15 μM tert-butyl hydroperoxide (t-BOOH, an organic peroxide) were added to the system where indicated; additionally, 1 mM ADP and 1 μg/mL oligomycin (Oligo) were added to induce and to cease oxidative phosphorylation, respectively, in experiments depicted in panels C and D. The mean (+SEM) of the time spent to recover the reduced state of NAD(P) following the addition of the t-BOOH load (i.e., the ability of mitochondria to scavenge peroxide) is shown in panel E (N = 10–14). These time-lapses were used to indirectly estimate the rates of peroxide removal in each group and experimental condition. Then, these data were plotted in a single graph in a manner that emphasizes the effects of ADP, HFD, *Nnt* mutation and their interaction on mitochondrial peroxide removal (panel F). The horizontal and vertical grey lines represent the extent of HFD effects on the variables represented on *x* and *y* axes, respectively. Within the same respiratory state: $^{**}P \leq 0.05$, $^{*}P \leq 0.01$ *vs.* genotype-matched chow-fed mice; $^{\#}P \leq 0.01$ *vs.* *Nnt*$^{+/+}$ mice given the same diet.

group (peroxide removal assayed in the presence of ADP) (Fig. 5**E**), which was in agreement with a study that observed HFD-induced PDH inhibition in *Nnt* wild type rodents [4]. Nevertheless, because of the NNT properties mentioned above and elsewhere [17,18], suppressed pyruvate oxidation via PDH is expected to limit peroxide removal only in mitochondria devoid of NNT or during respiratory states eliciting no net formation of NADPH via NNT, such as during ADP phosphorylation sustained by pyruvate oxidation [17]. Considering the latter condition, it is important to remind that ADP itself can promote PDH reactivation [46], lessening its prior HFD-induced inhibition and deleterious effects on peroxide removal. Molecular mechanisms of PDH inhibition by phosphorylation have been studied in different cell types and support the idea that oxidative stress affects PDH function [47,48]. A possible pathway leading to decreased PDH activity involves an interplay between inflammatory and redox signals that converge on activating kinases such as c-Jun N-terminal kinases (JNK) [48], ultimately resulting in the phosphorylation of PDH [47], which possess three different serine residues as targets [41]. A more specific mechanism of PDH phosphorylation has been revealed in a mouse model that expectedly also lacks functional *Nnt* [3]; this study showed that pyruvate dehydrogenase kinase 2 expression increases in response to a HFD and, in turn, promotes the phosphorylation and inhibition of PDH [3]. However, the mechanisms through which pyruvate dehydrogenase kinase 2 is upregulated remains unclear. The importance of PDH inhibition in NAFLD pathophysiology has been established by recent studies showing that PDH activation, by means of molecular or pharmacological suppression of PDH phosphorylation, significantly ameliorated metabolic control and hepatic steatosis in mice on HFD [3,11,12]. As these studies reported the use of mice that are expected to carry a *Nnt*-mutated genetic background (i.e., from the C57BL/6J substrain), our current findings suggest that the mechanisms underlying the improvement of metabolic control and NAFLD resulting from PDH activation [3,11,12]

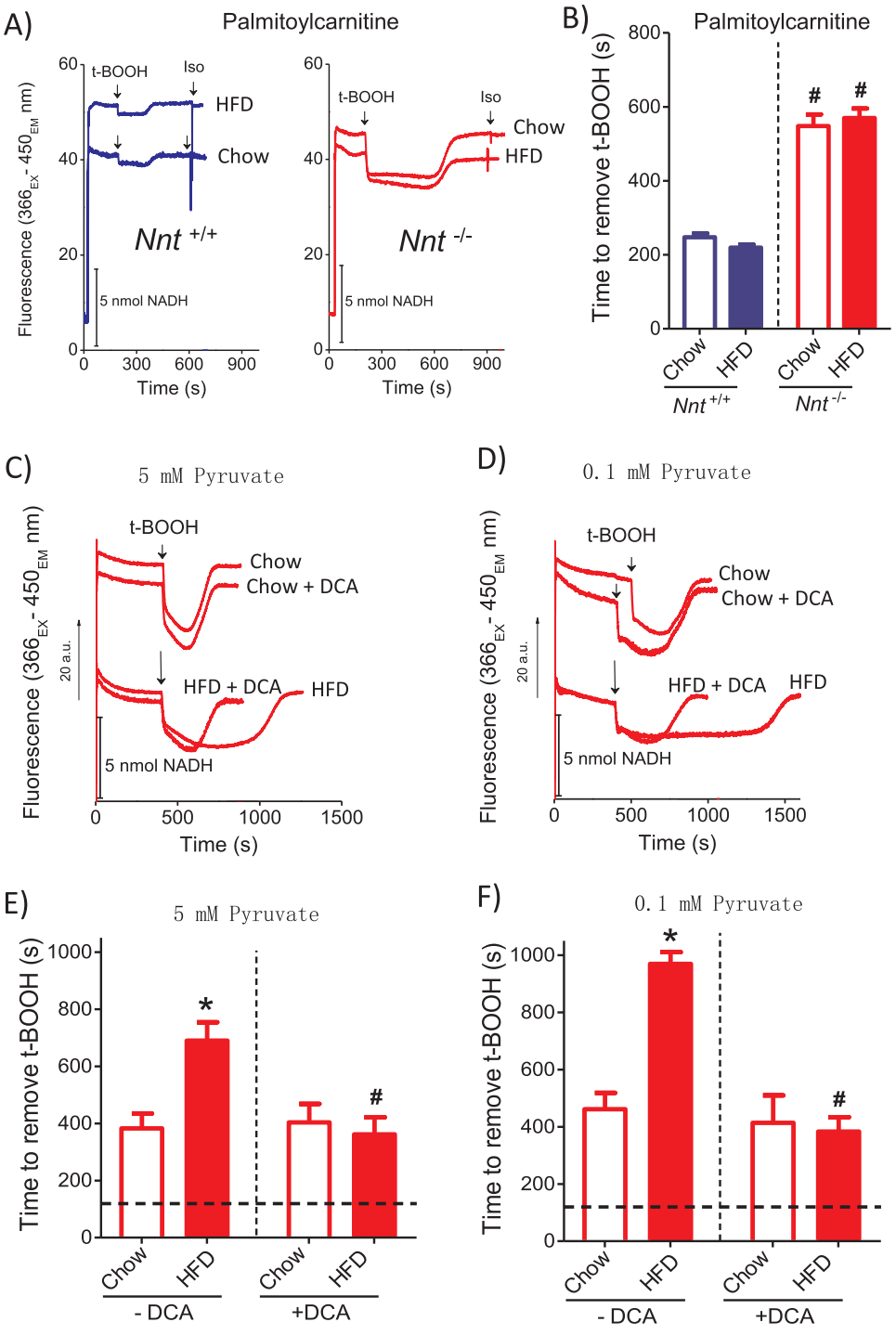

Fig. 6. Bypass or pharmacological reactivation of pyruvate dehydrogenase restored the peroxide removal capability of mitochondria from *Nnt*$^{-/-}$ mice under a high fat diet (HFD). The endogenous fluorescence NAD(P) in the reduced state was continuously monitored over time in mitochondria incubated in standard reaction medium supplemented with EGTA (300 μM) and malate (2.5 mM); some traces (HFD groups, Panels C and D) were displaced downwards in the plots to facilitate reading. Palmitoylcarnitine (15 μM) or pyruvate (0.1 or 5 mM) were the respiratory substrates, as specified in the panels. Palmitoylcarnitine was used to sustain substrate flux through the Krebs cycle independently of pyruvate dehydrogenase (PDH). One millimolar dichloroacetate (DCA, a PDH kinase inhibitor that results in PDH activation) was present ("+DCA") or absent (Control; "-DCA") from the beginning of the incubation in the experiments with pyruvate plus malate as substrates. The representative traces in panel A depict the addition of isolated mitochondria (0.5 mg/mL), 15 μM tert-butyl hydroperoxide (t-BOOH, an organic peroxide) and 1 mM isocitrate (a NAD(P) reductant) to the system where indicated, with palmitoylcarnitine plus malate as substrates. The time spent to recover the reduced state of NAD (P) following the addition of the t-BOOH load (i.e., the ability of mitochondria to scavenge peroxide) is shown in panel B. Similarly, panels C and D depict traces from the malate plus pyruvate conditions, where 10 μM t-BOOH was added to the system after a 5 min preincubation of mitochondria (0.5 mg/mL). The time spent to recover the reduced state of NAD (P) following the addition of the t-BOOH load is shown in panels E (N = 5–8) and F (N = 7–13). The horizontal dashed lines represent the values of chow-fed *Nnt*$^{+/+}$ mice mitochondria in the same experimental condition. DCA treatment did not modify t-BOOH removal capacity in mitochondria from *Nnt*$^{+/+}$ regardless of the diet (Supplementary material). $^{*}P \leq 0.01$ *vs.* chow-fed mice in the absence of DCA; $^{\#}P \leq 0.01$ *vs.* *Nnt*$^{-/-}$ on HFD in the absence DCA.

may include the restoration of redox balance in liver mitochondria and its broad beneficial secondary effects on related cellular processes.

As discussed above, we report here a redox-mediated interaction between the metabolic challenging condition imposed by a HFD and NNT, which results in PDH inhibition. Interestingly, Fisher-Wellman et al. [49] have recently identified another link between the functions of NNT and PDH, which is also redox mediated in skeletal muscle mitochondria from standard chow-fed mice. These authors reported an energy consuming redox circuit operating between PDH and NNT, based on the following rationale: the reductive pressure of pyruvate on PDH stimulates the production of H_2O_2 by this enzyme; the generated H_2O_2 will be detoxified at the expense of NADPH oxidation, which will result in stimulation of NNT activity, increased H^+ re-entry back to mitochondrial matrix and higher respiratory rate. Thus, PDH may be considered both a target that is affected by mitochondrial redox imbalance and a source of H_2O_2 contributing to redox imbalance under some conditions.

Along with results from studies on heart biology [30] and disease [50], the data presented here are seminal experimental evidences that the *Nnt* mutation by itself modified the results of an *in vivo* experimental intervention. Therefore, these findings are of pivotal importance, since research communities in various biomedical areas have increasingly become aware that a large contingent of experimental data have been obtained in diverse mouse models that carry the *Nnt* mutation from the C57BL/6J mouse substrain [11,22,25,39,42,45,51]. When the widely used C57BL/6J inbred mice substrain was discovered to bear a

Table 1
Contents of NADPH following t-BOOH-induced NADPH oxidation in liver mitochondria from *Nnt*$^{-/-}$ mice on a HFD.

Conditions	15 μM t-BOOH	NADPH (nmol/mg)
Malate + Pyruvate	no	1.97 ± 0.18
Malate + Pyruvate	yes	0.39 ± 0.03*
Malate + Pyruvate + ADP	yes	2.19 ± 0.33
Malate + Pyruvate + DCA	yes	1.91 ± 0.14
Malate + Palmitoylcarnitine	no	1.86 ± 0.17
Malate + Palmitoylcarnitine	yes	1.92 ± 0.24

Liver mitochondria from *Nnt*$^{-/-}$ mice on a HFD (0.5 mg/mL) were incubated in standard reaction medium supplemented with 300 μM EGTA. Respiratory substrates were either 2.5 mM malate plus 5 mM pyruvate or 2.5 mM malate plus 15 μM palmitoylcarnitine; also, ADP (1 mM) or DCA (1 mM) were absent or present in order to resemble the experiments depicted in Figs. 5D, 6A and 6C. The mitochondrial suspensions were pre-incubated for 7 min prior the addition of t-BOOH; 10–11 min afterwards, samples were withdrawn and enzymatically analyzed for reduced NADP levels. Data are means ± standard error (N = 4). * P < 0.01 compared to all other conditions.

spontaneous and homozygous loss-of-function *Nnt* mutation in 2005 [21,31], the basic biochemistry of NNT function had already been characterized, such that the reagents, products and cellular location of the NNT reaction were known [13,52]. The results from the first two studies reporting this *Nnt* mutation suggested that it could be linked to impaired glucose homeostasis [21] and an abnormal phenotype of genetically engineered mice [31]. Ever since, innumerable studies have continued to use mice carrying the C57BL/6J genetic background as models of metabolic diseases, including fatty liver diseases [11,22,39,42,45,51]. Undeniably, there is a scientific conundrum regarding the experimental use of *Nnt*-mutated mice as wild-type, which deserves attention from researchers [25,27,53,54].

In summary, we showed that the decrease in mitochondrial NADPH-dependent peroxide removal in the absence of functional NNT, due to *Nnt* mutation, altered the adaptations of liver mitochondria to a HFD. Notably, the interaction between HFD and the *Nnt* mutation resulted in redox imbalance, higher susceptibility to permeability transition pore opening and an inhibition of pyruvate oxidation via PDH in liver mitochondria, which was accompanied by an aggravation of NAFLD from simple steatosis to NASH. Thus, NNT seems to play a critical role in

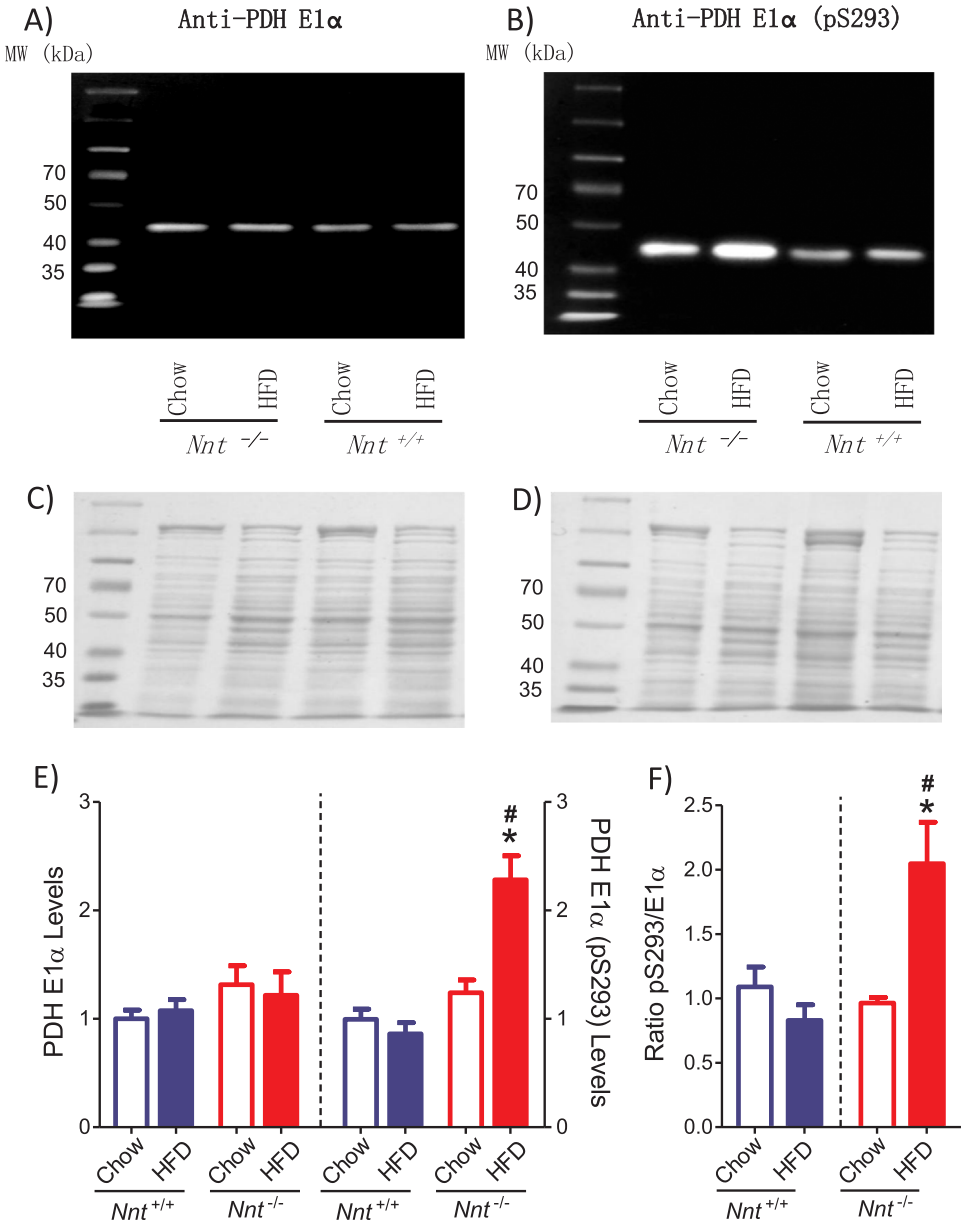

Fig. 7. A high fat diet (HFD) led to the phosphorylation of pyruvate dehydrogenase (PDH)-E1α subunit only in the liver mitochondria of *Nnt*$^{-/-}$ mice. Isolated mitochondria samples (50 μg) were probed for the relative levels of PDH-E1α (a subunit of the PDH complex) and serine^{293}-phosphorylated PDH-E1α by SDS-PAGE/western blot. Panels A and B show representative bands (~43 kDa, predicted) obtained with the primary antibodies against PDH-E1α and serine^{293}-phosphorylated PDH-E1α, respectively; molecular weight markers are on the left lanes. A protein loading control was evaluated by staining the membrane with Ponceau as demonstrated in panels C and D. Panel E shows the mean + SEM (N = 5–9) of the relative levels of PDH-E1α and serine^{293}-phosphorylated PDH-E1α, calculated as the optical density of the bands normalized by the optical density of their respective loading controls. The ratios between the levels of PDH-E1α and serine^{293}-phosphorylated PDH-E1α depict the PDH phosphorylation state in panel F (N = 5–9). $^{*}P \leq 0.01$ *vs.* genotype-matched chow-fed mice; $^{\#}P \leq 0.01$ *vs.* *Nnt*$^{+/+}$ mice given the same diet.

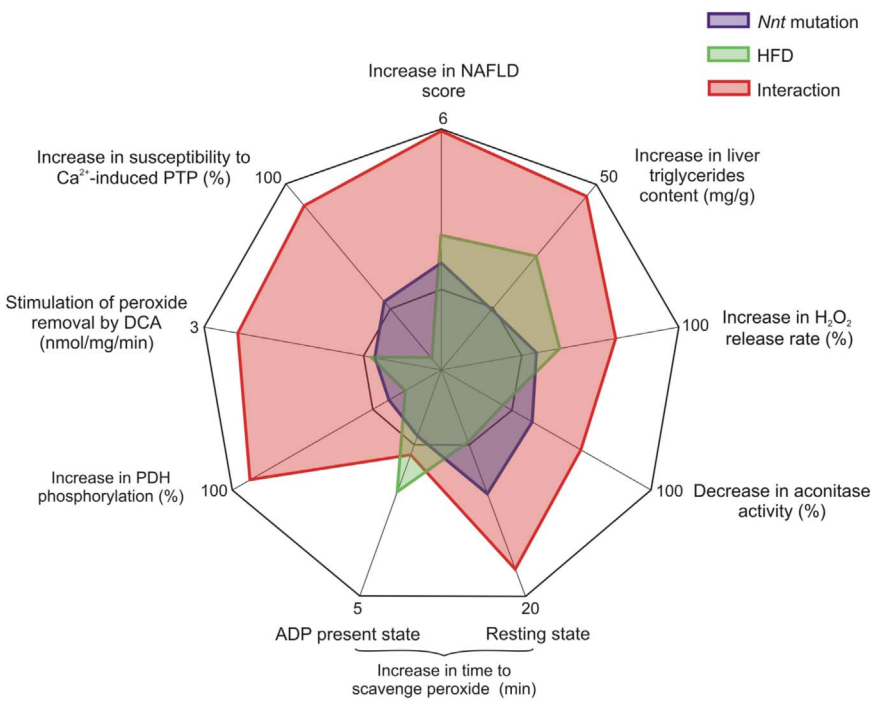

Fig. 8. Graphical summary of the effects of the *Nnt* mutation, high fat diet (HFD) and interaction between them on non-alcoholic fatty liver disease (NAFLD) and mitochondrial functions. The effects of *Nnt* mutation were the differences between the mean values observed in $Nnt^{+/+}$ and in $Nnt^{-/-}$ mice groups, both given a chow diet. The effects of HFD were the differences between the mean values observed in chow-fed $Nnt^{+/+}$ mice and in $Nnt^{+/+}$ mice on a HFD. The effects of the interaction between the *Nnt* mutation and a HFD were the differences between the mean values observed in chow-fed $Nnt^{+/+}$ mice and in $Nnt^{-/-}$ mice on a HFD. Each spoke of the radar chart is an axel representing the absolute or relative changes in a given variable; grid lines are shown at zero and maximal scale values only; the higher the distances from the zero line, the higher were the deleterious effects; values below zero indicate changes in opposite directions (i.e., of protection), and the only variable significantly altered in this direction was "Ca^{2+}-induced permeability transition (PTP)" in response to HFD. The changes in H_2O_2 release rate, aconitase activity, pyruvate dehydrogenase (PDH) phosphorylation and susceptibility to Ca^{2+}-induced PTP (measured using malate plus pyruvate as substrates) are expressed in percentages and their scale amplitudes vary between −50% and 100%; the changes in the other variables are expressed in absolute units with upper limits that are shown next to their axes (the origin of each axel is equal to its upper limit value multiplied by −0.5). All data used to build this radar chart were shown in Figs. 1–7. The NAFLD score was the sum of all histological grades depicted in Fig. 2.

counteracting mitochondrial redox imbalance and NAFLD following HFD. These findings implicate that mice models carrying mutated *Nnt*, such as C57BL/6J, can bias results and must not be overlooked when planning or interpreting studies on HFD-induced NAFLD.

Acknowledgments

We are thankful to Rosana A. T. Pereira from the laboratory of *Anatomia Patológica* (FCM/UNICAMP) for assisting with the preparation of liver slides for histological analyses.

Funding

This work was supported by the São Paulo Research Foundation (FAPESP, grant numbers 11/50400-0 and 13/07607-8). Fellowships were granted to TRF (from the Brazilian National Council for Scientific and Technological Development, CNPq #150546/2015-7), to AF (from FAPESP, #15/22063-0) and to JCR (from FAPESP, #14/02819-0).

Conflicts of interest

None

Appendix A. Supplementary material

Supplementary data associated with this article can be found in the online version at http://dx.doi.org/10.1016/j.freeradbiomed.2017.09.026.

References

[1] R.T. Hurt, C. Kulisek, L.A. Buchanan, S.A. McClave, The obesity epidemic: challenges, health initiatives, and implications for gastroenterologists, Gastroenterol. Hepatol. 6 (2011) 780–792.
[2] R. Buettner, J. Scholmerich, L.C. Bollheimer, High-fat diets: modeling the metabolic disorders of human obesity in rodents, Obesity 15 (2007) 798–808.
[3] Y. Go, J.Y. Jeong, N.H. Jeoung, J.H. Jeon, B.Y. Park, H.J. Kang, C.M. Ha, Y.K. Choi, S.J. Lee, H.J. Ham, B.G. Kim, K.G. Park, S.Y. Park, C.H. Lee, C.S. Choi, T.S. Park, W.N. Lee, R.A. Harris, I.K. Lee, Inhibition of pyruvate dehydrogenase kinase 2 protects against hepatic steatosis through modulation of TCA cycle anaplerosis and ketogenesis, Diabetes 65 (2016) 2876–2887.
[4] T.C. Alves, D.E. Befroy, R.G. Kibbey, M. Kahn, R. Codella, R.A. Carvalho, K. Falk Petersen, G.I. Shulman, Regulation of hepatic fat and glucose oxidation in rats with lipid-induced hepatic insulin resistance, Hepatology 53 (2011) 1175–1181.
[5] S. Satapati, B. Kucejova, J.A. Duarte, J.A. Fletcher, L. Reynolds, N.E. Sunny, T. He, L.A. Nair, K. Livingston, X. Fu, M.E. Merritt, A.D. Sherry, C.R. Malloy, J.M. Shelton, J. Lambert, E.J. Parks, I. Corbin, M.A. Magnuson, J.D. Browning, S.C. Burgess, Mitochondrial metabolism mediates oxidative stress and inflammation in fatty liver, J. Clin. Investig. 125 (2015) 4447–4462.
[6] T. Schroder, D. Kucharczyk, F. Bar, R. Pagel, S. Derer, S.T. Jendrek, A. Sunderhauf, A.K. Brethack, M. Hirose, S. Moller, A. Kunstner, J. Bischof, I. Weyers, J. Heeren, D. Koczan, S.M. Schmid, S. Divanovic, D.A. Giles, J. Adamski, K. Fellermann, H. Lehnert, J. Kohl, S. Ibrahim, C. Sina, Mitochondrial gene polymorphisms alter hepatic cellular energy metabolism and aggravate diet-induced non-alcoholic steatohepatitis, Mol. Metab. 5 (2016) 283–295.
[7] P.A. Kakimoto, A.J. Kowaltowski, Effects of high fat diets on rodent liver bioenergetics and oxidative imbalance, Redox Biol. 8 (2016) 216–225.
[8] V. Ribas, C. Garcia-Ruiz, J.C. Fernandez-Checa, Glutathione and mitochondria, Front. Pharmacol. 5 (2014) 151.
[9] K. Begriche, J. Massart, M.A. Robin, F. Bonnet, B. Fromenty, Mitochondrial adaptations and dysfunctions in nonalcoholic fatty liver disease, Hepatology 58 (2013) 1497–1507.
[10] S. Spahis, E. Delvin, J.M. Borys, E. Levy, Oxidative stress as a critical factor in nonalcoholic fatty liver disease pathogenesis, Antioxid. Redox Signal. 26 (2017) 519–541.
[11] B. Hwang, N.H. Jeoung, R.A. Harris, Pyruvate dehydrogenase kinase isoenzyme 4 (PDHK4) deficiency attenuates the long-term negative effects of a high-saturated fat diet, Biochem. J. 423 (2009) 243–252.
[12] S.C. Tso, X. Qi, W.J. Gui, C.Y. Wu, J.L. Chuang, I. Wernstedt-Asterholm, L.K. Morlock, K.R. Owens, P.E. Scherer, N.S. Williams, U.K. Tambar, R.M. Wynn, D.T. Chuang, Structure-guided development of specific pyruvate dehydrogenase kinase inhibitors targeting the ATP-binding pocket, J. Biol. Chem. 289 (2014) 4432–4443.
[13] J. Rydstrom, Mitochondrial NADPH, transhydrogenase and disease, Biochim. Biophys. Acta 1757 (2006) 721–726.
[14] T.R. Figueira, M.H. Barros, A.A. Camargo, R.F. Castilho, J.C. Ferreira, A.J. Kowaltowski, F.E. Sluse, N.C. Souza-Pinto, A.E. Vercesi, Mitochondria as a source of reactive oxygen and nitrogen species: from molecular mechanisms to human health, Antioxid. Redox Signal. 18 (2013) 2029–2074.
[15] A.J. Kowaltowski, R.F. Castilho, A.E. Vercesi, Mitochondrial permeability transition and oxidative stress, FEBS Lett. 495 (2001) 12–15.
[16] A.E. Vercesi, The participation of NADP, the transmembrane potential and the energy-linked NAD(P) transhydrogenase in the process of Ca2+ efflux from rat liver mitochondria, Arch. Biochem. Biophys. 252 (1987) 171–178.
[17] J.A. Ronchi, A. Francisco, L.A. Passos, T.R. Figueira, R.F. Castilho, The contribution of nicotinamide nucleotide transhydrogenase to peroxide detoxification is dependent on the respiratory state and counterbalanced by other sources of NADPH in liver mitochondria, J. Biol. Chem. 291 (2016) 20173–20187.
[18] J.A. Ronchi, T.R. Figueira, F.G. Ravagnani, H.C. Oliveira, A.E. Vercesi, R.F. Castilho, A spontaneous mutation in the nicotinamide nucleotide transhydrogenase gene of C57BL/6J mice results in mitochondrial redox abnormalities, Free Radic. Biol. Med. 63 (2013) 446–456.

[19] B.A. Paim, J.A. Velho, R.F. Castilho, H.C. Oliveira, A.E. Vercesi, Oxidative stress in hypercholesterolemic LDL (low-density lipoprotein) receptor knockout mice is associated with low content of mitochondrial NADP-linked substrates and is partially reversed by citrate replacement, Free Radic. Biol. Med. 44 (2008) 444–451.
[20] H.C. Oliveira, R.G. Cosso, L.C. Alberici, E.N. Maciel, A.G. Salerno, G.G. Dorighello, J.A. Velho, E.C. de Faria, A.E. Vercesi, Oxidative stress in atherosclerosis-prone mouse is due to low antioxidant capacity of mitochondria, FASEB J. 19 (2005) 278–280.
[21] A.A. Toye, J.D. Lippiat, P. Proks, K. Shimomura, L. Bentley, A. Hugill, V. Mijat, M. Goldsworthy, L. Moir, A. Haynes, J. Quarterman, H.C. Freeman, F.M. Ashcroft, R.D. Cox, A genetic and physiological study of impaired glucose homeostasis control in C57BL/6J mice, Diabetologia 48 (2005) 675–686.
[22] C. Poussin, M. Ibberson, D. Hall, J. Ding, J. Soto, E.D. Abel, B. Thorens, Oxidative phosphorylation flexibility in the liver of mice resistant to high-fat diet-induced hepatic steatosis, Diabetes 60 (2011) 2216–2224.
[23] A. Nicholson, P.C. Reifsnyder, R.D. Malcolm, C.A. Lucas, G.R. MacGregor, W. Zhang, E.H. Leiter, Diet-induced obesity in two C57BL/6 substrains with intact or mutant nicotinamide nucleotide transhydrogenase (Nnt) gene, Obesity 18 (2010) 1902–1905.
[24] A. Vitali, I. Murano, M.C. Zingaretti, A. Frontini, D. Ricquier, S. Cinti, The adipose organ of obesity-prone C57BL/6J mice is composed of mixed white and brown adipocytes, J. Lipid Res. 53 (2012) 619–629.
[25] D.A. Fontaine, D.B. Davis, Attention to background strain is essential for metabolic research: C57BL/6 and the International Knockout Mouse Consortium, Diabetes 65 (2016) 25–33.
[26] K. Mekada, K. Abe, A. Murakami, S. Nakamura, H. Nakata, K. Moriwaki, Y. Obata, A. Yoshiki, Genetic differences among C57BL/6 substrains, Exp. Anim. 58 (2009) 141–149.
[27] A. Kraev, Parallel universes of Black Six biology, Biol. Direct 9 (2014) 18.
[28] K.H. Fisher-Wellman, T.E. Ryan, C.D. Smith, L.A. Gilliam, C.T. Lin, L.R. Reese, M.J. Torres, P.D. Neufer, A Direct comparison of metabolic responses to high fat diet in C57BL/6J and C57BL/6NJ mice, Diabetes 65 (2016) 3249–3261.
[29] E. Rendina-Ruedy, K.D. Hembree, A. Sasaki, M.R. Davis, S.A. Lightfoot, S.L. Clarke, E.A. Lucas, B.J. Smith, A Comparative study of the metabolic and skeletal response of C57BL/6J and C57BL/6N mice in a diet-induced model of type 2 diabetes, J. Nutr. Metab. 2015 (2015) 758080.
[30] A. Kim, C.H. Chen, P. Ursell, T.T. Huang, Genetic modifier of mitochondrial superoxide dismutase-deficient mice delays heart failure and prolongs survival, Mamm. Genome 21 (2010) 534–542.
[31] T.T. Huang, M. Naeemuddin, S. Elchuri, M. Yamaguchi, H.M. Kozy, E.J. Carlson, C.J. Epstein, Genetic modifiers of the phenotype of mice deficient in mitochondrial superoxide dismutase, Hum. Mol. Genet. 15 (2006) 1187–1194.
[32] Y. Kamada, S. Kiso, Y. Yoshida, N. Chatani, T. Kizu, M. Hamano, M. Tsubakio, T. Takemura, H. Ezaki, N. Hayashi, T. Takehara, Estrogen deficiency worsens steatohepatitis in mice fed high-fat and high-cholesterol diet, Am. J. Physiol. Gastrointest. Liver Physiol. 301 (2011) G1031–G1043.
[33] M. Ganz, T. Csak, G. Szabo, High fat diet feeding results in gender specific steatohepatitis and inflammasome activation, World J. Gastroenterol. 20 (2014) 8525–8534.
[34] D.E. Kleiner, E.M. Brunt, M. Van Natta, C. Behling, M.J. Contos, O.W. Cummings, L.D. Ferrell, Y.C. Liu, M.S. Torbenson, A. Unalp-Arida, M. Yeh, A.J. McCullough, A.J. Sanyal, Design and validation of a histological scoring system for nonalcoholic fatty liver disease, Hepatology 41 (2005) 1313–1321.
[35] H. Chweih, R.F. Castilho, T.R. Figueira, Tissue and sex specificities in Ca(2+) handling by isolated mitochondria in conditions avoiding the permeability transition, Exp. Physiol. 100 (2015) 1073–1092.
[36] P.R. Gardner, D.D. Nguyen, C.W. White, Aconitase is a sensitive and critical target of oxygen poisoning in cultured mammalian cells and in rat lungs, Proc. Natl. Acad. Sci. USA 91 (1994) 12248–12252.
[37] Y. Chen, J. Cai, D.P. Jones, Mitochondrial thioredoxin in regulation of oxidant-induced cell death, FEBS Lett. 580 (2006) 6596–6602.
[38] H. Liu, J.P. Kehrer, The reduction of glutathione disulfide produced by t-butyl hydroperoxide in respiring mitochondria, Free Radic. Biol. Med. 20 (1996) 433–442.
[39] Y. Zhang, Z. Zhao, B. Ke, L. Wan, H. Wang, J. Ye, Induction of posttranslational modifications of mitochondrial proteins by ATP contributes to negative regulation of mitochondrial function, PLoS One 11 (2016) e0150454.
[40] C. Crewe, M. Kinter, L.I. Szweda, Rapid inhibition of pyruvate dehydrogenase: an initiating event in high dietary fat-induced loss of metabolic flexibility in the heart, PLoS One 8 (2013) e77280.
[41] M.J. Rardin, S.E. Wiley, R.K. Naviaux, A.N. Murphy, J.E. Dixon, Monitoring phosphorylation of the pyruvate dehydrogenase complex, Anal. Biochem. 389 (2009) 157–164.
[42] J.R. Mercer, E. Yu, N. Figg, K.K. Cheng, T.A. Prime, J.L. Griffin, M. Masoodi, A. Vidal-Puig, M.P. Murphy, M.R. Bennett, The mitochondria-targeted antioxidant MitoQ decreases features of the metabolic syndrome in ATM+/-/ApoE-/- mice, Free Radic. Biol. Med. 52 (2012) 841–849.
[43] M.M. Simon, S. Greenaway, J.K. White, H. Fuchs, V. Gailus-Durner, S. Wells, T. Sorg, K. Wong, E. Bedu, E.J. Cartwright, R. Dacquin, S. Djebali, J. Estabel, J. Graw, N.J. Ingham, I.J. Jackson, A. Lengeling, S. Mandillo, J. Marvel, H. Meziane, F. Preitner, O. Puk, M. Roux, D.J. Adams, S. Atkins, A. Ayadi, L. Becker, A. Blake, D. Brooker, H. Cater, M.F. Champy, R. Combe, P. Danecek, A. di Fenza, H. Gates, A.K. Gerdin, E. Golini, J.M. Hancock, W. Hans, S.M. Holter, T. Hough, P. Jurdic, T.M. Keane, H. Morgan, W. Muller, F. Neff, G. Nicholson, B. Pasche, L.A. Roberson, J. Rozman, M. Sanderson, L. Santos, M. Selloum, C. Shannon, A. Southwell, G.P. Tocchini-Valentini, V.E. Vancollie, H. Westerberg, W. Wurst, M. Zi, B. Yalcin, R. Ramirez-Solis, K.P. Steel, A.M. Mallon, M.H. de Angelis, Y. Herault, S.D. Brown, A comparative phenotypic and genomic analysis of C57BL/6J and C57BL/6N mouse strains, Genome Biol. 14 (2013) R82.
[44] J.T. Heiker, A. Kunath, J. Kosacka, G. Flehmig, A. Knigge, M. Kern, M. Stumvoll, P. Kovacs, M. Bluher, N. Kloting, Identification of genetic loci associated with different responses to high-fat diet-induced obesity in C57BL/6N and C57BL/6J substrains, Physiol. Genom. 46 (2014) 377–384.
[45] K. Gariani, K.J. Menzies, D. Ryu, C.J. Wegner, X. Wang, E.R. Ropelle, N. Moullan, H. Zhang, A. Perino, V. Lemos, B. Kim, Y.K. Park, A. Piersigilli, T.X. Pham, Y. Yang, C.S. Ku, S.I. Koo, A. Fomitchova, C. Canto, K. Schoonjans, A.A. Sauve, J.Y. Lee, J. Auwerx, Eliciting the mitochondrial unfolded protein response by nicotinamide adenine dinucleotide repletion reverses fatty liver disease in mice, Hepatology 63 (2016) 1190–1204.
[46] M.L. Pratt, T.E. Roche, Mechanism of pyruvate inhibition of kidney pyruvate dehydrogenasea kinase and synergistic inhibition by pyruvate and ADP, J. Biol. Chem. 254 (1979) 7191–7196.
[47] Q. Zhou, P.Y. Lam, D. Han, E. Cadenas, c-Jun N-terminal kinase regulates mitochondrial bioenergetics by modulating pyruvate dehydrogenase activity in primary cortical neurons, J. Neurochem. 104 (2008) 325–335.
[48] H. Kamata, S. Honda, S. Maeda, L. Chang, H. Hirata, M. Karin, Reactive oxygen species promote TNFalpha-induced death and sustained JNK activation by inhibiting MAP kinase phosphatases, Cell 120 (2005) 649–661.
[49] K.H. Fisher-Wellman, C.T. Lin, T.E. Ryan, L.R. Reese, L.A. Gilliam, B.L. Cathey, D.S. Lark, C.D. Smith, D.M. Muoio, P.D. Neufer, Pyruvate dehydrogenase complex and nicotinamide nucleotide transhydrogenase constitute an energy-consuming redox circuit, Biochem. J. 467 (2015) 271–280.
[50] A.G. Nickel, A. von Hardenberg, M. Hohl, J.R. Loffler, M. Kohlhaas, J. Becker, J.C. Reil, A. Kazakov, J. Bonnekoh, M. Stadelmaier, S.L. Puhl, M. Wagner, I. Bogeski, S. Cortassa, R. Kappl, B. Pasieka, M. Lafontaine, C.R. Lancaster, T.S. Blacker, A.R. Hall, M.R. Duchen, L. Kastner, P. Lipp, T. Zeller, C. Muller, A. Knopp, U. Laufs, M. Bohm, M. Hoth, C. Maack, Reversal of mitochondrial transhydrogenase causes oxidative stress in heart failure, Cell Metab. 22 (2015) 472–484.
[51] Y. Guo, M. Darshi, Y. Ma, G.A. Perkins, Z. Shen, K.J. Haushalter, R. Saito, A. Chen, Y.S. Lee, H.H. Patel, S.P. Briggs, M.H. Ellisman, J.M. Olefsky, S.S. Taylor, Quantitative proteomic and functional analysis of liver mitochondria from high fat diet (HFD) diabetic mice, Mol. Cell Proteom. 12 (2013) 3744–3758.
[52] J.B. Hoek, J. Rydstrom, Physiological roles of nicotinamide nucleotide transhydrogenase, Biochem. J. 254 (1988) 1–10.
[53] M. Bourdi, J.S. Davies, L.R. Pohl, Mispairing C57BL/6 substrains of genetically engineered mice and wild-type controls can lead to confounding results as it did in studies of JNK2 in acetaminophen and concanavalin A liver injury, Chem. Res. Toxicol. 24 (2011) 794–796.
[54] S.J. Navarro, T. Trinh, C.A. Lucas, A.J. Ross, K.G. Waymire, G.R. Macgregor, The C57BL/6J mouse strain background modifies the effect of a mutation in Bcl2l2, G3 (Bethesda) 2 (2012) 99–102.